

L_2 BN: Enhancing Batch Normalization by Equalizing the L_2 Norms of Features

Zhennan Wang Kehan Li Runyi Yu Yian Zhao Pengchong Qiao
 Chang Liu Fan Xu Xiangyang Ji Guoli Song Jie Chen

Abstract

In this paper, we analyze batch normalization from the perspective of discriminability and find the disadvantages ignored by previous studies: the difference in l_2 norms of sample features can hinder batch normalization from obtaining more distinguished inter-class features and more compact intra-class features. To address this issue, we propose a simple yet effective method to equalize the l_2 norms of sample features. Concretely, we l_2 -normalize each sample feature before feeding them into batch normalization, and therefore the features are of the same magnitude. Since the proposed method combines the l_2 normalization and batch normalization, we name our method L_2 BN. The L_2 BN can strengthen the compactness of intra-class features and enlarge the discrepancy of inter-class features. The L_2 BN is easy to implement and can exert its effect without any additional parameters or hyper-parameters. We evaluate the effectiveness of L_2 BN through extensive experiments with various models on image classification and acoustic scene classification tasks. The results demonstrate that the L_2 BN can boost the generalization ability of various neural network models and achieve considerable performance improvements.

1. Introduction

Batch Normalization (BN) [17] is a milestone in improving deep neural networks. Nonetheless, BN has some disadvantages. One of them is that BN does not perform well with a small batch size [45]. Another disadvantage is that BN is not suitable for sequence models [2], such as RNN [18], LSTM [10], GRU [4], and Transformer [44]. The information leakage [46] is also a shortcoming of BN, which means that the models may exploit mini-batch information rather than learn representations that generalize to individual samples [7]. From the robustness perspective, BN may increase adversarial vulnerability and decrease adversarial transferability [3]. As these drawbacks have been identified, there have been many approaches to address them to varying degrees [47, 16, 2, 46].

In this paper, we find that BN has other overlooked shortcomings. First, BN does not enlarge the discrepancy of

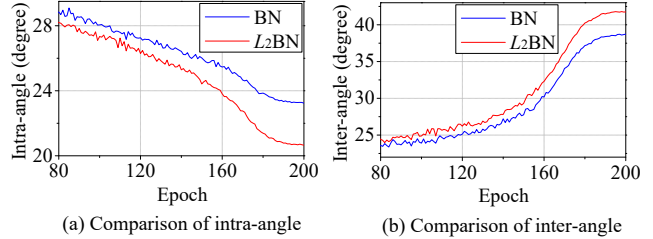


Figure 1. (a) The comparison of intra-angle curves indicates that the L_2 BN can enhance the intra-class compactness. (b) The comparison of inter-angle curves indicates that the L_2 BN can enlarge the inter-class discrepancy.

inter-class features to the maximum possible extent. Taking Figure 2 (b) and (c) as an example, after the BN, the minimum angle between pairwise class centers increases from 24.77° to 35.81° . However, the minimum angle can reach 120° theoretically. Second, BN makes the intra-class features less compact. Taking Figure 5 (a) as an example, the intra-class features are similar in orientation originally. After the transformation of BN, they are separated in direction. Through the forward pass of multiple layers, this intra-class separation may be magnified. To the best of our knowledge, we are the first to discover the disadvantages of BN from the perspective of discriminability.

To address these issues of BN, we propose a simple and intuitive approach. As shown in Figure 3, we just make the l_2 norms of features identical before feeding them into BN. Since our method combines the l_2 normalization and batch normalization, we call it L_2 BN. There are several advantages of L_2 BN: (a) It can continuously broaden the minimum angle between pairwise class centers, as shown in Figure 4. Therefore, the L_2 BN can enlarge the discrepancy of inter-class features. (b) The L_2 BN can eliminate the intra-class separation caused by the difference in l_2 norms of sample features, as shown in Figure 5 (b). (c) The L_2 BN is easy to implement without any extra parameters and hyper-parameters.

To verify the effect of L_2 BN, we adopt the measures of intra-class compactness and inter-class discrepancy used in ArcFace [6]. The intra-class compactness is measured by intra-angle, which is defined as the mean of angles across features w.r.t. their respective class feature centers. The inter-class discrepancy is measured by inter-angle, which

is defined as the mean of minimum angles between each class feature center and the others. We plot the intra-angle and the inter-angle of training data in Figure 1 (a) and (b) respectively, taking the ResNet-110 [9] model trained on CIFAR100 [19] as an example. During the whole training process, the L_2 BN model achieves a smaller intra-angle than the BN model consistently, indicating that the L_2 BN obtains more compact intra-class features. Furthermore, the L_2 BN model gradually gets a larger inter-angle than the BN model, indicating that the L_2 BN obtains more distinguished inter-class features. Overall, the L_2 BN is able to enhance the intra-class compactness and inter-class discrepancy simultaneously, and therefore the feature discrimination and generalization capability are strengthened.

In practice, the implementation of L_2 BN is very simple and requires only a few lines of code. To exhibit the effectiveness and generality of L_2 BN, we conduct extensive experiments with various classical convolutional neural networks on tasks of image classification and acoustic scene classification. For both tasks, we replace each BN layer in models with an L_2 BN layer. Experimental results show that the L_2 BN can generally improve the classification accuracy, decrease the intra-angle, and increase the inter-angle, which demonstrates that the L_2 BN can enhance the generalizability and the discriminability of neural networks. These experiments show that the L_2 BN is generally useful and can be used as an improved alternative to batch normalization in designing neural networks.

2. Related Work

Typical Normalization Methods. Since Batch Normalization (BN) was proposed by [17], various normalization methods have emerged. Recurrent Batch Normalization [5] applies BN to the hidden-to-hidden transition of recurrent neural networks, improving the generalization ability on various sequential problems. Layer Normalization [2] (LN) performs a similar normalization to BN, but on elements across the channel or feature dimension, mainly used in sequential models like plain RNN [33], LSTM [10], GRU [4], and Transformer [44]. Instance Normalization [43] (IN) normalizes activations per channel for individual samples, mainly used in image style transfer [15]. Positional Normalization [20] (PN) normalizes activations along the channel dimension for generative networks. Group Normalization [45] (GN) is a middle way between IN and LN. GN divides the channels into groups and implements normalization within each group, mainly used in computer vision [9, 8].

In addition to these, some methods explore combinations of these methods. Batch Group Normalization [50] uses the mixed statistics of GN and BN. Batch-Channel Normalization [29] wraps BN and GN in a module. Divisive Normalization [32] proposes a unified view of LN and BN.

Switchable Normalization [23] is a learning-to-normalize method, which switches between IN, LN, and BN by learning their importance weights in an end-to-end manner. To avoid redundant computation, Sparse Switchable Normalization [37] selects only one normalizer for each normalization layer with the help of SparsestMax, a sparse version of softmax. Batch-Instance Normalization [25] learns to adaptively combine BN and IN. IBN [27] uses IN in some channels or layers and BN in other channels or layers. XBNBlock [14] replaces the BN with batch-free normalization, like GN, in the bottleneck block of residual-style networks.

Instead of subtracting the mean and divided by the sample standard deviation, there exist other operations to do normalization. L^1 batch normalization [11] replaces the sample standard deviation with the average absolute deviation from the mean, thus improving numerical stability in low-precision implementations as well as providing computational and memory benefits substantially. Like IN, Filter Response Normalization [40] also normalizes the activations of each channel of a single feature map, but only divides by the mean squared norm without subtracting the mean value. Similarly, Power Normalization [38] divides by the mean squared norm along the batch dimension and is mainly used in Transformer for NLP tasks. RMSNorm [49] preserves the re-scaling invariance property of LN but eschews the re-centering invariance property, making it computationally simpler and more efficient than LN. ScaleNorm [26] further simplifies RMSNorm by setting only one uniform scale parameter for each layer.

Rather than on activations, some methods normalize weights. Weight Normalization [35] aims at decoupling the magnitudes of those weight vectors from their directions by introducing a specific magnitude parameter for each weight vector. Weight Standardization [30] standardizes the weights in the convolutional layers to accelerate the training, which is motivated by [36] that shows the smoothing effects of BN on activations.

Improvements of Batch Normalization. Despite so many normalization methods, BN is still the most widely used and generally effective for convolutional neural networks [9, 13]. However, the original BN comes with some noticeable disadvantages. The most known one is the poor performance when the batch size is relatively small [45], due to the unstable batch statistics. To address this issue, Batch Renormalization [16] uses population statistics instead of batch statistics while subtly retaining the backpropagation of batch statistics. To further stabilize training, Moving Average Batch Normalization [47] substitutes batch statistics by moving average statistics in both forward and backward propagation. EvalNorm [41] estimates the corrected normalization statistics during evaluation to address the performance degradation of BN. Based on Taylor poly-

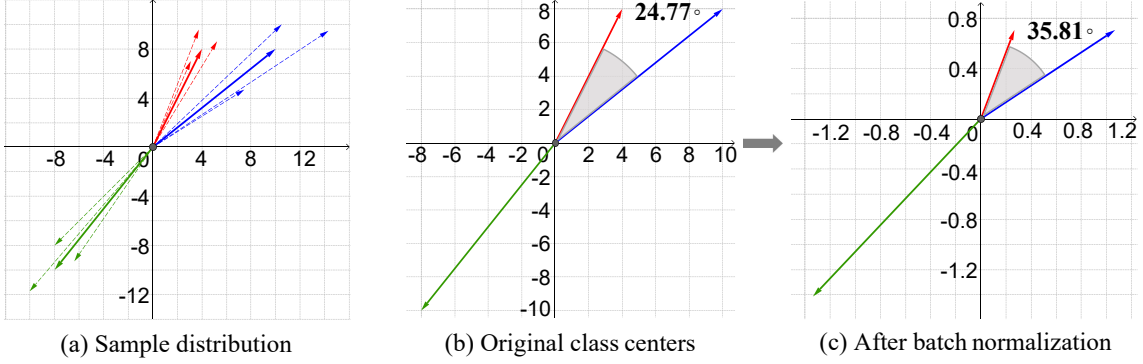


Figure 2. The influence of BN on inter-class features. (a) The dotted vectors with different colors represent features of different classes, and the solid vectors denote the class centers. (b) Since the analysis is on inter-class features, we only consider the class centers for the convenience of analysis. The minimum angle between pairwise class centers is 24.77° . (c) After BN, the minimum angle gets enlarged up to 35.81° and will not change even with more identity mapping layers, indicating that BN can not maximize the discrepancy of inter-class features.

nomials, Cross-Iteration Batch Normalization [48] jointly utilizes multiple recent iterations to enhance the estimation quality of batch statistics. Our proposed L_2 BN is also an improvement of BN. However, unlike the above methods, L_2 BN is developed to address the issues of inter-class feature discrepancy and intra-class feature compactness caused by BN, which is ignored by previous work.

3. Method

In this section, we first define the proposed L_2 BN. Then we analyze the advantages of L_2 BN. Finally, we describe the implementation details of L_2 BN.

3.1. The Proposed L_2 BN

Assuming the input data is $\mathbf{X} \in R^{b \times d}$, where b denotes the batch size and d denotes the feature dimension of input samples, the proposed L_2 BN is formulated as:

$$\hat{\mathbf{X}}_i = \frac{\mathbf{X}_i}{\|\mathbf{X}_i\|}, \quad (1)$$

$$BN(\hat{\mathbf{X}}_i) = \frac{\gamma}{\delta} \odot (\hat{\mathbf{X}}_i - \mu) + \beta, \quad (2)$$

where $\mathbf{X}_i \in R^d$ denotes the i -th sample feature, $\hat{\mathbf{X}}_i$ denotes the l_2 -normalized feature vector, $\|\cdot\|$ denotes the Euclidean norm, $\mu \in R^d$ and $\delta \in R^d$ denote the sample mean and uncorrected sample standard deviation of l_2 -normalized \mathbf{X} along the batch dimension respectively, $\gamma \in R^d$ and $\beta \in R^d$ are learnable affine parameters, and \odot is the element-wise multiplication between two vectors. That is, we perform l_2 normalization for each feature vector before feeding them into BN, and thus the magnitudes of feature vectors become identical.

To make the method more intuitive, we visualize the whole process in Figure 3. Since the proposed method

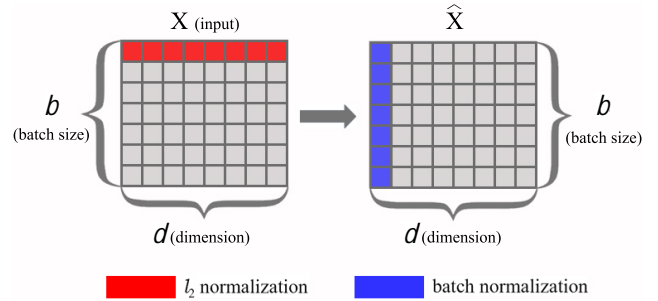


Figure 3. The illustration of L_2 BN.

combines the l_2 normalization and batch normalization, we name our method L_2 BN. As shown in Figure 3, L_2 BN does not attempt to modify the BN itself, as BN is very helpful for the optimization of neural networks [17, 36]. L_2 BN just implements an additional l_2 normalization to make the input samples of BN have equal magnitudes, which leaves the vector orientations as the only difference between samples. As analyzed below, this simple but intuitive method can address the issues of inter-class discrepancy and intra-class compactness caused by BN.

3.2. Analysis of L_2 BN

This section explores the influence of L_2 BN on the inter-class discrepancy and intra-class compactness.

Enlarging the Discrepancy of Inter-class Features. To facilitate the analysis, we consider the sample distribution in 2-D space, as shown in Figure 2 (a). Given that this is for analyzing the inter-class discrepancy, we only consider the class center for each class as in Figure 2 (b). For simplicity, we assume that the γ equals one and β equals zero in BN, and each layer in neural network is an identity mapping.

Because of centering and scaling the elements along the batch dimension [17, 28], the minimum angle between pairwise class centers gets enlarged after the transformation of BN, as shown in Figure 2 (c). In other words, BN

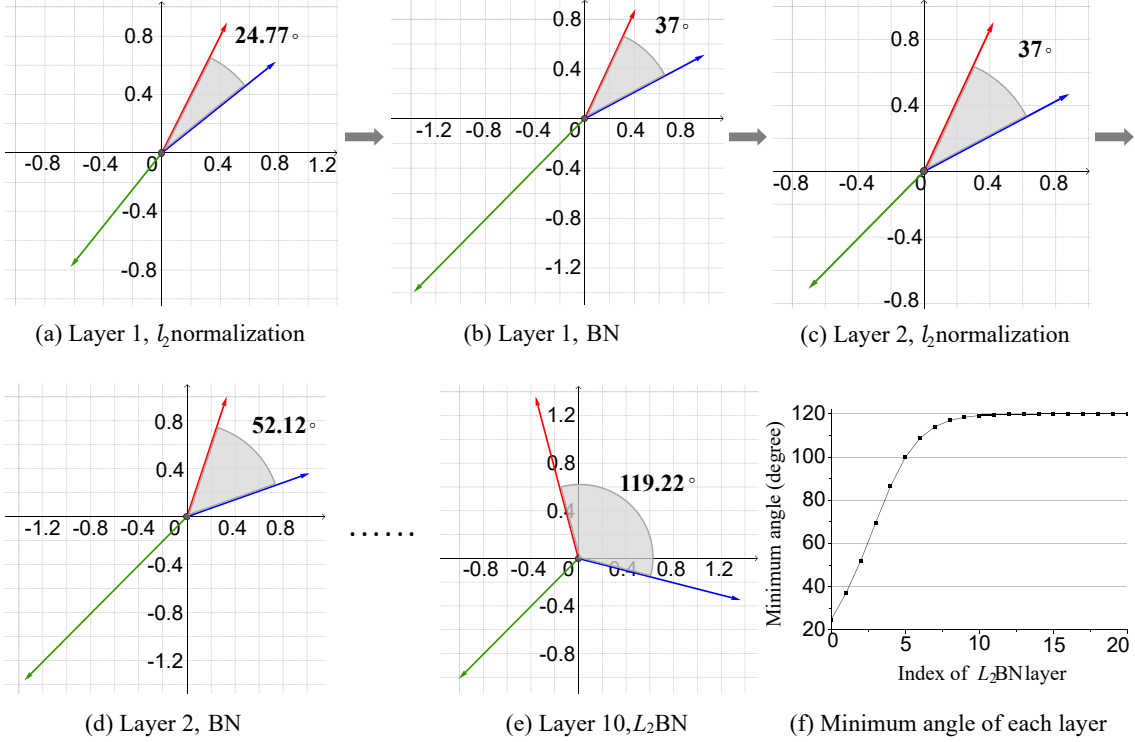


Figure 4. The influence of L_2 BN on inter-class features. Assume that the layers are identity mappings. (a) After the l_2 normalization of L_2 BN within the first layer, the minimum angle remains the same, but the Euclidean norms become identical. (b) After the batch normalization of L_2 BN within the first layer, the minimum angle gets enlarged up to 37° . (c) After the l_2 normalization of L_2 BN within the second layer, the Euclidean norms become the same again. (d) After the batch normalization of L_2 BN within the second layer, the minimum angle gets enlarged up to 52.12° . (e) After the L_2 BN within the tenth layer, the minimum angle gets enlarged up to 119.22° , indicating that L_2 BN can enlarge the discrepancy of inter-class features. (f) The minimum angle continues to grow as the number of layers increases until it reaches the maximum.

separates the inter-class features to some extent. We argue that this is one of the reasons why BN can facilitate the optimization of neural networks. However, since the sample mean μ and sample standard deviation δ have become 0 and 1 respectively after a single BN operation, the sample distribution will not change even after multiple BN operations. Therefore, BN can not separate the inter-class features further, as we can see in Figure 2 (c).

In the case of using L_2 BN, we visualize the evolution of class centers in Figure 4. Compared with BN, the advantage of L_2 BN is that it can continuously expand the minimum angle between pairwise class centers, which benefits from the additional l_2 normalization. As an illustration, the Euclidean norms of class centers are not identical after the L_2 BN within the first identity mapping layer in Figure 4 (a) and (b). Thus, the l_2 normalization can still change the sample distribution within the second identity mapping layer in Figure 4 (c). In turn, the l_2 normalization destroys the distribution state of zero mean and unit variance, which allows the subsequent BN to remain valid. Therefore, the minimum angle between pairwise class centers is further enlarged, as shown in Figure 4 (d). After several identity

mapping layers, L_2 BN can separate the inter-class features to the maximal extent, as in Figure 4 (e) and (f). As a result, the proposed L_2 BN can achieve a larger inter-class discrepancy than BN.

Enhancing the Compactness of Intra-class Features. In addition to the impact on inter-class features, the difference in the Euclidean norms of features also affects the compactness of intra-class features after BN. For intra-class features, we assume that their orientations are similar and expect them to maintain similar after BN. This is a reasonable assumption, since orientations represent semantic information [22] and intra-class features belong to the same semantic class. To illustrate the problem intuitively, we take Figure 5 (a) as an example, in which the b_1 and b_2 vectors belong to the same class. After the transformation of BN, the intra-class feature vectors with similar orientations but different Euclidean norms are further separated. Through the forward propagation of multiple layers, this separation of intra-class features may be magnified, which leads to less compact intra-class features. The proposed L_2 BN makes the Euclidean norms identical before feeding the features into BN and thus eliminates the impact of difference in

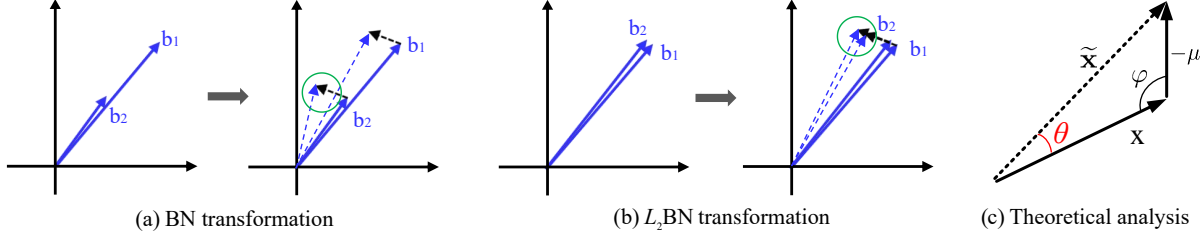


Figure 5. The influence of BN and L_2 BN on intra-class features. The b_1 and b_2 vectors belong to the same class, the angle between them is very small but the difference in Euclidean norms is large. The short black dotted vector represents the opposite vector of the shared mean vector μ . For simplicity, we do not consider the influence of sample standard deviation. (a) After BN, the directional difference between b_1 and b_2 becomes larger, resulting in less compact intra-class features. (b) Due to the additional l_2 normalization, the directional difference between b_1 and b_2 is still small after the L_2 BN transformation. (c) The angle θ is determined by μ , φ , and the Euclidean length of \mathbf{x} . The \mathbf{x} denotes the vector before BN and the $\tilde{\mathbf{x}}$ denotes the vector after BN. The φ denotes the angle between \mathbf{x} and μ .

Euclidean norms, which is a simple and intuitive approach to address this issue as shown in Figure 5 (b).

Besides the above intuitive analysis, we do a brief theoretical analysis. The analysis schematic is shown in Figure 5 (c). The μ is calculated per batch and is shared for each sample vector. Once the orientation of \mathbf{x} is given, the angle φ between \mathbf{x} and μ is knowable. Also, the θ is related to the Euclidean length of \mathbf{x} . In summary, the θ can be formulated as $\theta = f(\mu, \varphi, \|\mathbf{x}\|)$. Evidently, the variance of $\|\mathbf{x}\|$ can be passed to the θ . The L_2 BN eliminates the variance of $\|\mathbf{x}\|$ through an additional l_2 normalization. Therefore, the variance of θ is reduced and the compactness of intra-class features is enhanced.

3.3. Implementation

Although the above analysis focuses on the classification layer, the L_2 BN can also be applied to the hidden layers. We experimentally verify that applying L_2 BN to all layers achieves the greatest accuracy improvement in the Experiments Section 4.1. For image tasks like image classification, 2D convolution is commonly used. In this case, we perform l_2 normalization on the whole feature map of each sample, because the sample feature is represented by the whole feature map under this setting. That is, Equation (1) is replaced with:

$$\hat{\mathbf{X}}_i = \frac{\mathbf{X}_i}{\max(\sqrt{\sum_{j=1}^{C \times H \times W} \mathbf{X}_{ij}^2}, \epsilon)}, \quad \text{or} \quad (3)$$

$$\hat{\mathbf{X}}_i = \frac{\sqrt{C \times H \times W} * \mathbf{X}_i}{\max(\sqrt{\sum_{j=1}^{C \times H \times W} \mathbf{X}_{ij}^2}, \epsilon)},$$

where ϵ is a very small number added for division stability. The C , H , and W denote the channel number, height, and width of the feature map respectively. Because of the subsequent BN operation, multiplying by $\sqrt{C \times H \times W}$ does not affect the output of L_2 BN in theory. But by doing so, it can prevent floating point underflow in the case of large feature size.

4. Experiments

4.1. Image Classification

Experimental Settings. We verify the advantages of L_2 BN over BN by conducting image classification experiments using convolutional networks. We experiment on the CIFAR100 dataset [19] and the ImageNet-1K dataset [34]. On CIFAR100, we employ various classic networks as the backbone models, including ResNet-20\32\44\56\110 [9], DenseNet [13] with 40 layers and a growth rate of 12 denoted by DenseNet-40-12, DenseNet-BC [13] with 100 layers and a growth rate of 12 denoted by DenseNet-BC-100-12, VGG-19 [39] with BN, and RegNet-Y [31]. On ImageNet-1K, we evaluate our method with ResNet-50, ResNet-101, ResNeXt-50 ($32 \times 4d$), and ResNeXt-101 ($32 \times 4d$).

For CIFAR100, we report the mean and standard deviation of the best accuracy over 5 runs with random seeds ranging from 121 to 125, reducing the impacts of random variations. For ImageNet-1K, we fix the random seed to 1. For a fair comparison, not only the L_2 BN models but also their BN counterparts are trained from scratch, so our results may be slightly different from the ones presented in the original papers due to different random seeds, software, and hardware settings. Other training settings and hyper-parameters are detailed in the supplementary materials.

Main Results and Analysis. Table 1 and Table 2 show the comparison results of the models and their L_2 BN versions on CIFAR100 and ImageNet-1K, respectively.

In terms of accuracy, the L_2 BN can improve all the backbone models to varying degrees, regardless of the CIFAR100 or the ImageNet-1K dataset. For example, the L_2 BN can boost the accuracy of ResNet-56 by about 1% on CIFAR100 and ResNet-50 by about 0.6% on ImageNet-1K. It is worth emphasizing that the L_2 BN achieves the improvements without any additional parameters or hyper-parameters. Due to the pre-attached l_2 normalization, the accuracy improvement benefits from the elimination of the difference in l_2 norms of sample features. To intuitively

Model	BN/ L_2 BN	Accuracy(%) \uparrow	Intra and Inter angles (degree)			IIR	
			Intra(train) \downarrow	Intra(test) \downarrow	Inter \uparrow	train \downarrow	test \downarrow
ResNet-20	BN	69.70 \pm 0.30	28.15	29.04	21.70	1.297	1.338
ResNet-20	L_2 BN	70.17 \pm 0.20	27.61	28.69	22.31	1.238	1.286
ResNet-32	BN	71.40 \pm 0.20	27.43	28.75	23.65	1.160	1.216
ResNet-32	L_2 BN	71.75 \pm 0.21	26.90	28.39	24.41	1.102	1.163
ResNet-44	BN	72.53 \pm 0.25	27.06	28.56	24.80	1.091	1.152
ResNet-44	L_2 BN	73.10 \pm 0.14	26.28	28.05	25.85	1.016	1.085
ResNet-56	BN	72.88 \pm 0.25	24.76	28.91	34.09	0.726	0.848
ResNet-56	L_2 BN	73.92 \pm 0.20	22.90	27.73	35.92	0.638	0.772
ResNet-110	BN	74.82 \pm 0.20	23.45	28.78	38.98	0.602	0.739
ResNet-110	L_2 BN	75.32 \pm 0.44	20.57	27.00	41.87	0.491	0.645
DenseNet-40-12	BN	75.17 \pm 0.27	27.45	29.21	23.54	1.166	1.241
DenseNet-40-12	L_2 BN	75.36 \pm 0.18	27.62	29.57	24.99	1.105	1.183
DenseNet-BC-100-12	BN	77.44 \pm 0.20	31.07	33.07	28.11	1.105	1.176
DenseNet-BC-100-12	L_2 BN	77.87 \pm 0.10	30.59	33.07	31.28	0.978	1.057
VGG-19	BN	73.77 \pm 0.50	13.32	27.89	58.81	0.226	0.474
VGG-19	L_2 BN	73.99 \pm 0.44	12.05	27.01	59.14	0.204	0.457
RegNet-Y	BN	78.21 \pm 0.29	25.07	32.69	57.94	0.433	0.564
RegNet-Y	L_2 BN	78.88 \pm 0.24	21.39	30.23	59.30	0.361	0.510

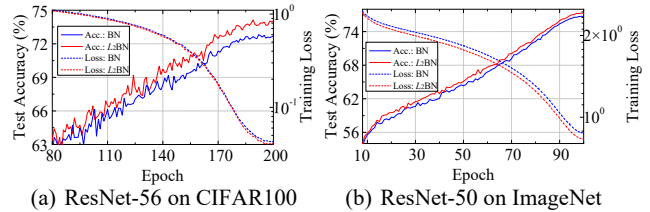
Table 1. Classification results on CIFAR100. We show the accuracy as “mean \pm std”. The IIR denotes the Intra-angle and Inter-angle Ratio, as defined in Equation (7).

Model	BN/ L_2 BN	Accuracy(%)
ResNet-50	BN	76.74
ResNet-50	L_2 BN	77.32
ResNet-101	BN	78.43
ResNet-101	L_2 BN	78.81
ResNeXt-50($32 \times 4d$)	BN	77.86
ResNeXt-50($32 \times 4d$)	L_2 BN	78.43
ResNeXt-101($32 \times 4d$)	BN	79.14
ResNeXt-101($32 \times 4d$)	L_2 BN	79.40

Table 2. Classification results on ImageNet-1K.

illustrate the effectiveness of L_2 BN, we plot the training curves of ResNet-56 on CIFAR100 and ResNet-50 on ImageNet-1K in Figure 6. The L_2 BN can get persistently higher classification accuracy and slightly smaller training loss than the BN baseline.

In Section 3.2, we analyze that the improvement in accuracy is due to the ability of L_2 BN to enhance intra-class compactness and inter-class discrepancy. In this part, we demonstrate this claim through extensive experiments. To measure the intra-class compactness and inter-class discrepancy quantitatively, we adopt the measures used in ArcFace [6]. The intra-class compactness is measured by the mean of angles across features with respect to their respective class feature centers, denoted as intra-angle. The inter-class discrepancy is measured by the mean of minimum angles between each class feature center and the other class feature centers, denoted as inter-angle. To be



(a) ResNet-56 on CIFAR100 (b) ResNet-50 on ImageNet
Figure 6. The comparison of training curves. The L_2 BN is persistently effective.

more clear, we give the formulations of intra-angle and inter-angle:

$$\mathbf{c}_i = \frac{1}{N_i} \sum_{j=1}^{N_i} \frac{\mathbf{x}_{ij}}{\|\mathbf{x}_{ij}\|}, \quad (4)$$

$$intra-angle = \frac{1}{\sum_{i=1}^C N_i} \sum_{i=1}^C \sum_{j=1}^{N_i} \arccos \left(\frac{\mathbf{x}_{ij} \mathbf{c}_i^T}{\|\mathbf{x}_{ij}\| \|\mathbf{c}_i\|} \right), \quad (5)$$

$$inter-angle = \frac{1}{C} \sum_{i=1}^C \min_{j \in [1, C], j \neq i} \arccos \left(\frac{\mathbf{c}_i \mathbf{c}_j^T}{\|\mathbf{c}_i\| \|\mathbf{c}_j\|} \right), \quad (6)$$

where $\mathbf{x}_{ij} \in R^{1 \times d}$ denotes the j -th sample feature vector of the i -th class, N_i denotes the number of samples belonging to the i -th class, $\mathbf{c}_i \in R^{1 \times d}$ denotes the feature center vector of the i -th class, and C denotes the number of classes.

We calculate the intra-angle of training data, the intra-angle of test data, and the inter-angle. The inter-angle refers to the one of training data, and we don’t calculate the inter-

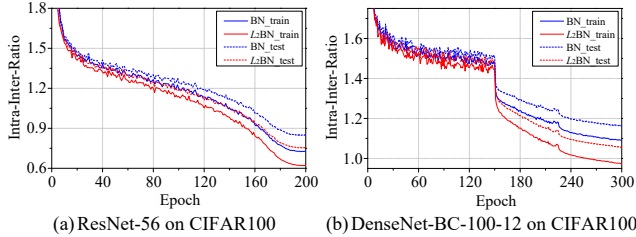


Figure 7. The comparison of *IIR* curves. On both training data and test data, L_2 BN achieves consistently smaller *IIR*.

angle of test data. We argue that the inter-angle of test data is meaningless because the image classification is a closed-set task. For the same reason, we use the class feature centers computed on the training set for the calculation of intra-angle, whether the intra-angle is of training data or test data. Note that the intra-angle and inter-angle are only meaningful for the classification layer. The results in Table 1 show that the intra-angle is reduced after using the L_2 BN either on training data or on test data, for most of the models except the DenseNet. But for all models, the inter-angle gets enlarged. This demonstrates that the L_2 BN can make the intra-class features more compact and the inter-class features more separable. Therefore, the L_2 BN can enhance the discriminative ability of neural networks, which is the reason for the accuracy improvement.

Given the relative relationship between intra-class compactness and inter-class discrepancy, using either intra-angle or inter-angle alone is not sufficient to evaluate the discriminability of a model. For that reason, we define the Intra-angle and Inter-angle Ratio, abbreviated as *IIR*, as follows:

$$IIR = \frac{\text{intra-angle}}{\text{inter-angle}}. \quad (7)$$

The *IIR* is a unified metric to evaluate the intra-class compactness and the inter-class discrepancy, the smaller the better. We use the unified *IIR* to verify the effect of L_2 BN. For all the backbones, the L_2 BN can always achieve significantly smaller *IIR* on both training data and test data, as shown in Table 1. To be more rigorous, we compare the *IIR* of BN and L_2 BN throughout the training process in Figure 7. We can see that the L_2 BN can continuously get smaller *IIR*, demonstrating the advantages of L_2 BN.

It is worth mentioning that the types of backbones used here are diverse, including models with skip connection like ResNet [9] and DenseNet [13], models without skip connection like VGG [39], and models searched by Neural Architecture Search like RegNet [31]. This indicates that, as a simple plug-and-play module, the L_2 BN is shown to be architecture-agnostic and produce persistent performance improvement. Therefore, the key advantage of L_2 BN highlighted in this paper is not the significance but the robustness and generalizability.

Choice of Feature Normalization. In the Method Sec-

Methods	Accuracy(%) \uparrow	<i>IIR</i>	
		train \downarrow	test \downarrow
BN(baseline)	72.88 \pm 0.25	0.726	0.848
LNBN	73.57 \pm 0.20	0.674	0.802
INBN	69.34 \pm 0.29	0.739	0.870
PNBN	72.49 \pm 0.17	0.714	0.846
L_2 BN(ours)	73.92\pm0.20	0.638	0.772

Table 3. Ablation of possible alternatives to l_2 normalization in L_2 BN using ResNet-56 on CIFAR100.

tion 3, we employ the l_2 normalization on the whole feature map of each sample by default. To justify our choice, we also evaluate in Table 3 other possible alternatives to l_2 normalization such as Layer Normalization [2], Instance Normalization [43], and Position Normalization [20], denoted by LNBN, INBN, and PNBN, respectively.

We observe that the INBN and PNBN get much poorer performance than L_2 BN, in terms of both accuracy and *IIR*. We argue that it is the entire feature map that represents the sample feature, whether the Instance Normalization or the Position Normalization destroys the sample-level feature information. The Layer Normalization is also performed on the whole feature map. Compared with the l_2 normalization, the main difference is that Layer Normalization has a centering operation. From the analysis in Figure 4 and Figure 5, the centering operation is unnecessary for the intra-class compactness and inter-class discrepancy. Moreover, the centering operation changes the orientation of feature vector and thus may change what the feature vector can represent [17]. To address this, Layer Normalization in the original paper [2] employs a learned affine transformation to adaptively compensate for the possible information loss. However, the subsequent Batch Normalization makes the learned affine transformation of Layer Normalization ineffective in LNBN. Therefore, the information loss caused by Layer Normalization can not be effectively compensated. The l_2 normalization does not change the orientation of feature vector and therefore does not related to the semantic information loss [22, 21]. The results in Table 3 also prove that both the accuracy and the *IIR* of LNBN are inferior to those of L_2 BN. In summary, compared with these possible alternatives, l_2 normalization is the best choice.

Applying L_2 BN to Different Layers. As described in Section 3.3, the L_2 BN is applicable to all layers. To confirm this point, we study the effect of L_2 BN applied to different parts of neural networks, as shown in Table 4. Even if the L_2 BN is only used for part of the neural network, the accuracy can be improved to varying degrees. However, the accuracy is enhanced to the greatest extent when applying L_2 BN to all layers. This indicates that the L_2 BN is effective for both the output layer and the hidden layers, and the

L_2 BN	Accuracy(%)
None (baseline)	72.88±0.25
Only classification layer	73.04±0.27
ResStage 1	73.59±0.27
ResStage 2-3	73.43±0.17
All layers	73.92±0.20

Table 4. Ablation of applying L_2 BN to different layers using ResNet-56 on CIFAR100.

effects can be accumulated.

Comparison with Other Normalization Methods. This section compares L_2 BN with several existing variants of Batch Normalization, including Layer Normalization (LN) [2], Instance Normalization (IN) [43], Group Normalization (GN) [45], Switchable Normalization (SN) [23], Batch-Channel Normalization (BCN) [29], and Batch-Instance Normalization (BIN) [25]. For GN, we test settings with the channel-per-group (cpg) values of 4 and 8. For BCN, we set the number of groups to $\min\{32, (\text{the number of channels})/4\}$, as in the original paper [29]. The results are shown in Table 5. For LN, IN, and GN, they abandon the batch statistics and thus perform worse than BN in popular training settings [45]. SN, BCN, and BIN can be used to address the problem of poor performance of BN when the mini-batch size is very small. However, their performance in popular training settings is on par with or worse than BN. In contrast, the L_2 BN can still enhance BN when the mini-batch size is not small. Overall, the L_2 BN performs better than these normalization methods without any hyper-parameters.

Methods	Accuracy(%) \uparrow	<i>IIR</i>	
		train \downarrow	test \downarrow
BN(baseline) [17]	72.88±0.25	0.726	0.848
LN [2]	69.88±0.15	0.877	0.982
IN [43]	69.77±0.20	0.737	0.871
GN-cpg4 [45]	70.35±0.19	0.746	0.881
GN-cpg8 [45]	70.68±0.51	0.773	0.895
SN [23]	72.85±0.17	0.691	0.816
BCN [29]	72.90±0.20	0.795	0.909
BIN [25]	70.83±0.14	0.809	0.937
L_2 BN(ours)	73.92±0.20	0.638	0.772

Table 5. Comparison with other normalization methods using ResNet-56 on CIFAR100.

4.2. Acoustic Scene Classification

Experimental Settings. To further verify the effectiveness of our proposed method, we conduct experiments on the acoustic scene classification task. We experiment on the TUT Urban Acoustic Scenes 2020 Mobile Development dataset [42], which consists of 10-seconds audio segments from 10 acoustic scenes and contains in total of 64 hours of audio. The task we choose is a subtask of the acoustic

Model	BN/ L_2 BN	Accuracy(%)
ResNet-17	BN	72.51
ResNet-17	L_2 BN	72.64
FCNN	BN	69.17
FCNN	L_2 BN	70.55
fsFCNN	BN	71.19
fsFCNN	L_2 BN	72.44

Table 6. Results of Acoustic Scene Classification.

scene classification in the challenge on detection and classification of acoustic scenes and events (DCASE) [1]. The goal is to classify the audio into 10 distinct specific acoustic scenes, including airport, public square and urban park, etc.

We employ three CNN-based architectures as backbone models, including ResNet-17 [24], FCNN [12], and fsFCNN [12]. The optimizer is SGD with a cosine-decay-restart learning rates scheduler, in which the maximum and minimum learning rates are 0.1 and 1e-5 respectively. We train the ResNet-17 for 126 epochs and the FCNN and fsFCNN for 255 epochs. All of them are trained with a batch size of 32. For a fair comparison, we train both the L_2 BN models and the corresponding BN models from scratch under the same configurations.

Results. Table 6 shows the comparison results of the baseline models and their L_2 BN models on the acoustic scene classification task. For all three baseline models, the corresponding L_2 BN models can boost the accuracy under the same configurations. Specifically, L_2 BN can achieve a significant accuracy improvement of more than 1% for FCNN and fsFCNN. Together with the results of image classification experiments, we conclude that the L_2 BN is effective for different domains, which indicates that our proposed method is scalable and general.

5. Conclusion

In this paper, we propose a strong substitute for batch normalization, the L_2 BN, which makes the l_2 norms of sample features identical before feeding them into BN. Our analysis and experiments reveal that the proposed L_2 BN can facilitate intra-class compactness and inter-class discrepancy. Besides, the characteristic of requiring no additional parameters and hyper-parameters makes it easy to use. We evaluate the effect of L_2 BN on image classification and acoustic scene classification tasks with various deep neural networks, demonstrating its effectiveness and generalizability. As a simple but effective operation, we believe that L_2 BN can be integrated into a wide range of application scenarios as a plug-and-play module without any tuning.

References

- [1] Challenge on detection and classification of acoustic scenes and events, 2020. <https://dcase.community/challenge2020/index>. 8
- [2] Jimmy Lei Ba, Jamie Ryan Kiros, and Geoffrey E Hinton. Layer normalization. *arXiv preprint arXiv:1607.06450*, 2016. 1, 2, 7, 8
- [3] Philipp Benz, Chaoning Zhang, and In So Kweon. Batch normalization increases adversarial vulnerability and decreases adversarial transferability: A non-robust feature perspective. In *Proceedings of the IEEE/CVF International Conference on Computer Vision*, pages 7818–7827, 2021. 1
- [4] Kyunghyun Cho, Bart Van Merriënboer, Dzmitry Bahdanau, and Yoshua Bengio. On the properties of neural machine translation: Encoder-decoder approaches. *arXiv preprint arXiv:1409.1259*, 2014. 1, 2
- [5] Tim Cooijmans, Nicolas Ballas, César Laurent, Çağlar Gülçehre, and Aaron Courville. Recurrent batch normalization. *arXiv preprint arXiv:1603.09025*, 2016. 2
- [6] Jiankang Deng, Jia Guo, Niannan Xue, and Stefanos Zafeiriou. Arcface: Additive angular margin loss for deep face recognition. In *Proceedings of the IEEE Conference on Computer Vision and Pattern Recognition*, pages 4690–4699, 2019. 1, 6
- [7] Kaiming He, Haoqi Fan, Yuxin Wu, Saining Xie, and Ross Girshick. Momentum contrast for unsupervised visual representation learning. In *Proceedings of the IEEE/CVF conference on computer vision and pattern recognition*, pages 9729–9738, 2020. 1
- [8] Kaiming He, Georgia Gkioxari, Piotr Dollár, and Ross Girshick. Mask r-cnn. In *Proceedings of the IEEE international conference on computer vision*, pages 2961–2969, 2017. 2
- [9] Kaiming He, Xiangyu Zhang, Shaoqing Ren, and Jian Sun. Deep residual learning for image recognition. In *Proceedings of the IEEE conference on computer vision and pattern recognition*, pages 770–778, 2016. 2, 5, 7
- [10] Sepp Hochreiter and Jürgen Schmidhuber. Long short-term memory. *Neural computation*, 9(8):1735–1780, 1997. 1, 2
- [11] Elad Hoffer, Ron Banner, Itay Golan, and Daniel Soudry. Norm matters: efficient and accurate normalization schemes in deep networks. *Advances in Neural Information Processing Systems*, 31, 2018. 2
- [12] Hu Hu, Chao-Han Huck Yang, Xianjun Xia, Xue Bai, Xin Tang, Yajian Wang, Shutong Niu, Li Chai, Juanjuan Li, Hongning Zhu, Feng Bao, Yuanjun Zhao, Sabato Marco Siniscalchi, Yannan Wang, Jun Du, and Chin-Hui Lee. Device-robust acoustic scene classification based on two-stage categorization and data augmentation, 2020. 8
- [13] Gao Huang, Zhuang Liu, Laurens Van Der Maaten, and Kilian Q Weinberger. Densely connected convolutional networks. In *Proceedings of the IEEE conference on computer vision and pattern recognition*, pages 4700–4708, 2017. 2, 5, 7
- [14] Lei Huang, Yi Zhou, Tian Wang, Jie Luo, and Xianglong Liu. Delving into the estimation shift of batch normalization in a network. In *Proceedings of the IEEE/CVF Conference on Computer Vision and Pattern Recognition*, pages 763–772, 2022. 2
- [15] Xun Huang and Serge Belongie. Arbitrary style transfer in real-time with adaptive instance normalization. In *Proceedings of the IEEE international conference on computer vision*, pages 1501–1510, 2017. 2
- [16] Sergey Ioffe. Batch renormalization: Towards reducing minibatch dependence in batch-normalized models. In *Advances in neural information processing systems*, pages 1945–1953, 2017. 1, 2
- [17] Sergey Ioffe and Christian Szegedy. Batch normalization: Accelerating deep network training by reducing internal covariate shift. In *International Conference on Machine Learning*, pages 448–456, 2015. 1, 2, 3, 7, 8
- [18] Michael I Jordan. Serial order: A parallel distributed processing approach. In *Advances in psychology*, volume 121, pages 471–495. Elsevier, 1997. 1
- [19] Alex Krizhevsky. Learning multiple layers of features from tiny images. Technical report, Master’s thesis, University of Tront, 2009. 2, 5
- [20] Boyi Li, Felix Wu, Kilian Q Weinberger, and Serge Belongie. Positional normalization. *Advances in Neural Information Processing Systems*, 32, 2019. 2, 7
- [21] Weiyang Liu, Zhen Liu, Zhiding Yu, Bo Dai, Rongmei Lin, Yisen Wang, James M Rehg, and Le Song. Decoupled networks. In *Proceedings of the IEEE Conference on Computer Vision and Pattern Recognition*, pages 2771–2779, 2018. 7
- [22] Weiyang Liu, Yan-Ming Zhang, Xingguo Li, Zhiding Yu, Bo Dai, Tuo Zhao, and Le Song. Deep hyperspherical learning. In *Advances in neural information processing systems*, pages 3950–3960, 2017. 4, 7
- [23] Ping Luo, Jiamin Ren, Zhanglin Peng, Ruimao Zhang, and Jingyu Li. Differentiable learning-to-normalize via switchable normalization. *arXiv preprint arXiv:1806.10779*, 2018. 2, 8
- [24] MD McDonnell and W. Gao. Acoustic scene classification using deep residual networks with late fusion of separated high and low frequency paths. In *ICASSP 2020 - 2020 IEEE International Conference on Acoustics, Speech and Signal Processing (ICASSP)*, 2020. 8
- [25] Hyeonseob Nam and Hyo-Eun Kim. Batch-instance normalization for adaptively style-invariant neural networks. *Advances in Neural Information Processing Systems*, 31, 2018. 2, 8
- [26] Toan Q Nguyen and Julian Salazar. Transformers without tears: Improving the normalization of self-attention. *arXiv preprint arXiv:1910.05895*, 2019. 2
- [27] Xingang Pan, Ping Luo, Jianping Shi, and Xiaoou Tang. Two at once: Enhancing learning and generalization capacities via ibn-net. In *Proceedings of the European Conference on Computer Vision (ECCV)*, pages 464–479, 2018. 2
- [28] Xianbiao Qi and Lei Zhang. Face recognition via centralized coordinate learning. *arXiv preprint arXiv:1801.05678*, 2018. 3
- [29] Siyuan Qiao, Huiyu Wang, Chenxi Liu, Wei Shen, and Alan Yuille. Micro-batch training with batch-channel

- normalization and weight standardization. *arXiv preprint arXiv:1903.10520*, 2019. 2, 8
- [30] Siyuan Qiao, Huiyu Wang, Chenxi Liu, Wei Shen, and Alan Yuille. Weight standardization. *arXiv preprint arXiv:1903.10520*, 2019. 2
- [31] Ilija Radosavovic, Raj Prateek Kosaraju, Ross Girshick, Kaiming He, and Piotr Dollár. Designing network design spaces. In *Proceedings of the IEEE/CVF Conference on Computer Vision and Pattern Recognition*, pages 10428–10436, 2020. 5, 7
- [32] Mengye Ren, Renjie Liao, Raquel Urtasun, Fabian H Sinz, and Richard S Zemel. Normalizing the normalizers: Comparing and extending network normalization schemes. *arXiv preprint arXiv:1611.04520*, 2016. 2
- [33] David E Rumelhart, Geoffrey E Hinton, and Ronald J Williams. Learning representations by back-propagating errors. *nature*, 323(6088):533–536, 1986. 2
- [34] Olga Russakovsky, Jia Deng, Hao Su, Jonathan Krause, Sanjeev Satheesh, Sean Ma, Zhiheng Huang, Andrej Karpathy, Aditya Khosla, Michael Bernstein, et al. Imagenet large scale visual recognition challenge. *International journal of computer vision*, 115(3):211–252, 2015. 5
- [35] Tim Salimans and Durk P Kingma. Weight normalization: A simple reparameterization to accelerate training of deep neural networks. In *Advances in Neural Information Processing Systems*, pages 901–909, 2016. 2
- [36] Shibani Santurkar, Dimitris Tsipras, Andrew Ilyas, and Aleksander Madry. How does batch normalization help optimization? In *Advances in Neural Information Processing Systems*, pages 2483–2493, 2018. 2, 3
- [37] Wenqi Shao, Tianjian Meng, Jingyu Li, Ruimao Zhang, Yudian Li, Xiaogang Wang, and Ping Luo. Ssn: Learning sparse switchable normalization via sparsestmax. In *Proceedings of the IEEE Conference on Computer Vision and Pattern Recognition*, pages 443–451, 2019. 2
- [38] Sheng Shen, Zhewei Yao, Amir Gholami, Michael Mahoney, and Kurt Keutzer. Powernorm: Rethinking batch normalization in transformers. In *International Conference on Machine Learning*, pages 8741–8751. PMLR, 2020. 2
- [39] Karen Simonyan and Andrew Zisserman. Very deep convolutional networks for large-scale image recognition. In *International Conference on Learning Representations*, 2015. 5, 7
- [40] Saurabh Singh and Shankar Krishnan. Filter response normalization layer: Eliminating batch dependence in the training of deep neural networks. In *Proceedings of the IEEE/CVF Conference on Computer Vision and Pattern Recognition*, pages 11237–11246, 2020. 2
- [41] Saurabh Singh and Abhinav Shrivastava. Evalnorm: Estimating batch normalization statistics for evaluation. In *Proceedings of the IEEE/CVF International Conference on Computer Vision*, pages 3633–3641, 2019. 2
- [42] H Toni, M Annamaria, and V Tuomas. Tau urban acoustic scenes 2020 mobile development dataset [data set]. *Zenodo*, 2020. 8
- [43] Dmitry Ulyanov, Andrea Vedaldi, and Victor Lempitsky. Instance normalization: The missing ingredient for fast stylization. *arXiv preprint arXiv:1607.08022*, 2016. 2, 7, 8
- [44] Ashish Vaswani, Noam Shazeer, Niki Parmar, Jakob Uszkoreit, Llion Jones, Aidan N Gomez, Łukasz Kaiser, and Illia Polosukhin. Attention is all you need. *Advances in neural information processing systems*, 30, 2017. 1, 2
- [45] Yuxin Wu and Kaiming He. Group normalization. In *Proceedings of the European Conference on Computer Vision (ECCV)*, pages 3–19, 2018. 1, 2, 8
- [46] Yuxin Wu and Justin Johnson. Rethinking” batch” in batchnorm. *arXiv preprint arXiv:2105.07576*, 2021. 1
- [47] Junjie Yan, Ruosi Wan, Xiangyu Zhang, Wei Zhang, Yichen Wei, and Jian Sun. Towards stabilizing batch statistics in backward propagation of batch normalization. *arXiv preprint arXiv:2001.06838*, 2020. 1, 2
- [48] Zhuliang Yao, Yue Cao, Shuxin Zheng, Gao Huang, and Stephen Lin. Cross-iteration batch normalization. In *Proceedings of the IEEE/CVF Conference on Computer Vision and Pattern Recognition*, pages 12331–12340, 2021. 3
- [49] Biao Zhang and Rico Sennrich. Root mean square layer normalization. *Advances in Neural Information Processing Systems*, 32, 2019. 2
- [50] Xiao-Yun Zhou, Jiacheng Sun, Nanyang Ye, Xu Lan, Qijun Luo, Bo-Lin Lai, Pedro Esperanca, Guang-Zhong Yang, and Zhenguo Li. Batch group normalization. *arXiv preprint arXiv:2012.02782*, 2020. 2

Supplementary Material

A Training Settings for Image Classification Experiments

Dataset	Model	LR	LR Scheduler	WD	BS	Epochs	Warm-up
CIFAR100	ResNet	0.1	cosine, min_lr=0	5e-4	128	200	None
	DenseNet	0.1	[150, 225], gamma=0.1	1e-4	64	300	None
	VGG	0.1	cosine, min_lr=0	5e-4	128	200	None
	RegNet	0.5	cosine, min_lr=0	5e-4	512	200	5 epochs
ImageNet	ResNet	0.2	cosine, min_lr=0	5e-5	256	100	None
	ResNeXt	0.2	cosine, min_lr=0	5e-5	256	100	None

Table 1: Experimental settings on CIFAR100 and ImageNet. LR denotes learning rate, WD denotes weight decay, and BS denotes batch size.

The optimizer is SGD [2] with a Nesterov momentum [3] of 0.9. The simple data augmentation in [1] is used in all the experiments of this part. Besides, the training of RegNet uses *mixup* [5] with $\alpha = 0.5$ and label smoothing [4] with a smoothing parameter of 0.1. Other hyper-parameters and settings are detailed in Table 1, which are basically the same as those in the original papers.

B More IIR Curves for Image Classification Experiments

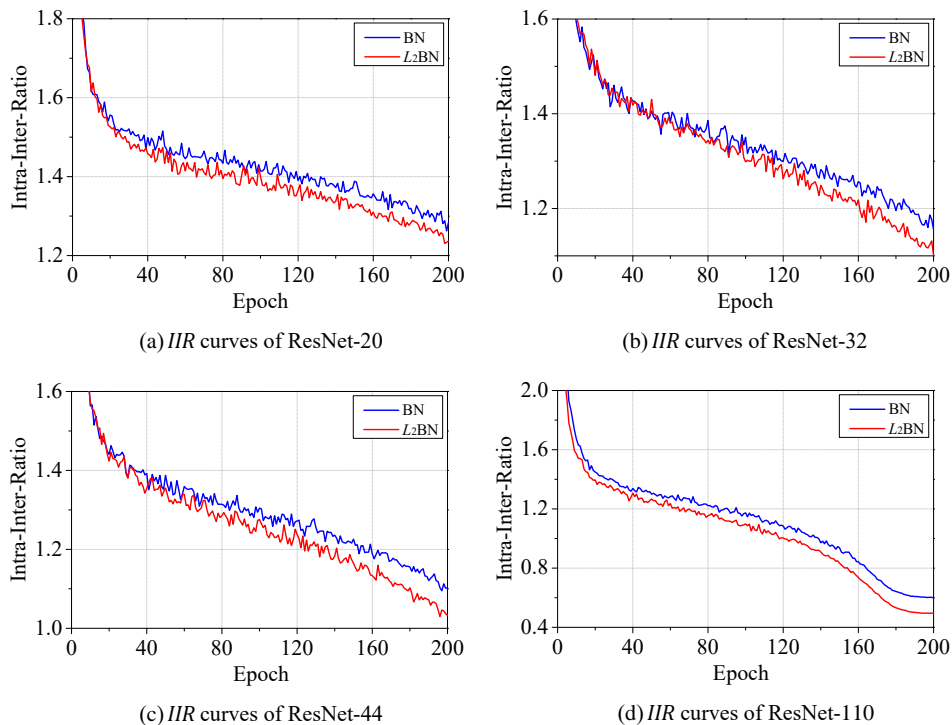


Figure 1: The comparison of IIR curves on training data of CIFAR100. L_2 BN achieves consistently smaller IIR across the whole training.

Figure 1 shows more IIR comparisons between BN and L_2 BN. The L_2 BN achieves consistently smaller IIR across the whole training process, which enhances the advantages of L_2 BN.

References

- [1] Chen-Yu Lee, Saining Xie, Patrick Gallagher, Zhengyou Zhang, and Zhuowen Tu. Deeply-supervised nets. In *Artificial Intelligence and Statistics*, pages 562–570, 2015.
- [2] David E Rumelhart, Geoffrey E Hinton, and Ronald J Williams. Learning representations by back-propagating errors. *nature*, 323(6088):533–536, 1986.
- [3] Ilya Sutskever, James Martens, George Dahl, and Geoffrey Hinton. On the importance of initialization and momentum in deep learning. In *International conference on machine learning*, pages 1139–1147. PMLR, 2013.
- [4] Christian Szegedy, Vincent Vanhoucke, Sergey Ioffe, Jon Shlens, and Zbigniew Wojna. Rethinking the inception architecture for computer vision. In *Proceedings of the IEEE conference on computer vision and pattern recognition*, pages 2818–2826, 2016.
- [5] Hongyi Zhang, Moustapha Cisse, Yann N Dauphin, and David Lopez-Paz. mixup: Beyond empirical risk minimization. *arXiv preprint arXiv:1710.09412*, 2017.